Redfield stoichiometry in Arabian Sea subsurface waters

Axel Hupe

Institut für Biogeochemie und Meereschemie, Universität Hamburg, Hamburg, Germany

Johannes Karstensen

Institut für Meereskunde, Universität Hamburg, Hamburg, Germany

Abstract. A linear inverse mixing model is applied to hydrographic, nutrient, and carbon data collected during Joint Global Ocean Flux Study and World Ocean Circulation Experiment cruises in 1995 to estimate the $\Delta C_{org}/\Delta N/\Delta P/\Delta Si/-\Delta O_2$ remineralization ratios within the Arabian Sea between 550 and 4500 m. The observed concentrations are separated into mixing fractions of source water masses and changes caused by remineralization processes, while the effect of denitrification is considered. In contrast to earlier investigations, diapycnal mixing, which plays an important role in dissolved matter fluxes in the Arabian Sea, is accounted for. The ratios are found to be variable with depth, especially in the upper 2000 m of the water column. We suppose that in general nutrients are released faster than carbon dioxide during remineralization. The $\Delta C_{org}/\Delta C_{inorg}$ decrease from $\sim$4 $\pm$ 1 at 550 m to 2 $\pm$ 0.2 at 2000 m and 1.2 $\pm$ 0.3 at 4000 m, suggesting that the dissolution of calcium carbonate above the calcite lysocline is a potentially important process within the Arabian Sea.

1. Introduction

Particulate organic matter (POM) in the ocean is formed by phytoplankton photosynthesis in the sunlit surface layer by taking up dissolved inorganic carbon (DIC) and nutrients. Fresh POM includes carbon, nitrogen, and phosphorus in the elemental ratio of 106/16/1 [*Redfield et al.*, 1963], which is found to be consistent throughout the world ocean [e.g. *Copin-Monteguet and Copin-Monteguet*, 1983; *Toggweiler*, 1993]. Recently, *Anderson* [1995] proposed a revised "Redfield" formula for the composition of marine algae with respect to the oxygen and hydrogen content:

$$106 \ CO_2 + 16 \ HNO_3 + H_3PO_4 + 78 \ H_2O \rightarrow$$
$$(C_{106}H_{175}O_{42}N_{16}P) + 150 \ O_2. \quad (1)$$
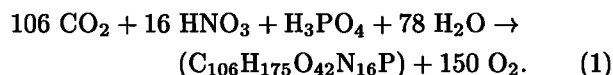
Part of the POM is exported out of the euphotic zone and is remineralized in subsurface waters, whereby DIC and nutrients are released again, while oxygen is consumed. In areas of upwelling, DIC and nutrients are returned to the surface layer. This cycle is referred to as the "biological CO_2 pump." As the biological

fixed DIC in the exported organic matter is replenished from the atmospheric reservoir, the DIC released during remineralization in the interior of the ocean reflects the drawdown of atmospheric CO_2 via the biological pump. This amount is commonly assessed by converting the biological changes in the concentrations of nutrients or apparent oxygen utilization (AOU) into the release of DIC using the stoichiometric ratio found in surface phytoplankton. These molecular ratios, often called the Redfield ratio, are of importance for many biological and chemical studies in oceanography such as far calculating "NO" [*Broecker*, 1974], estimating the anthropogenic CO_2 signal [e.g., *Brewer*, 1978; *Gruber et al.*, 1996] or for modeling the global carbon cycle [e.g., *Maier-Reimer*, 1993].

The determination of the stoichiometric ratios of carbon, nitrogen, phosphorus, and oxygen is basically differentiated into two approaches. The first strategy is based on the analysis of particulate organic matter [e.g., *Anderson*, 1995; *Honjo et al.*, 1982; *Knauer et al.*, 1979; *Martin et al.*, 1987; *Redfield et al.*, 1963]. The second method is to look at the stoichiometric ratios from oceanic chemical data, i.e., the change in nutrient and carbon concentrations as a result of remineralization processes [e.g., *Anderson and Sarmiento*, 1994; *Minster and Boulahdid*, 1987; *Shaffer*, 1996; *Shaffer et al.*, 1999; *Takahashi et al.*, 1985]. The "classical" $\Delta C_{org}/\Delta N/\Delta P/-\Delta O_2$ ratio of 106/16/1/138 [*Red-*

field et al., 1963] is based on the elemental composition of plankton protoplasm [*Fleming*, 1940], while the AOU value was inferred from stoichiometric constraints. Generally, it is not evident that the elements released to seawater during the degradation of organic matter reflect the composition of planktonic biomass because of preferentially remineralization of certain elements with depth [e.g., *Knauer et al.*, 1979; *Parsons et al.*, 1984; *Sambrotto et al.*, 1993; *Toggweiler*, 1993] and regional effects on the biogeochemical cycling. In summary, at present there exist two distinct views about stoichiometric ratios of remineralization. The first point of view, mainly based on the results of particulate matter analysis in the ocean interior (including *Shaffer* [1996] and *Shaffer et al.* [1999]), states that there is a considerable vertical fractionation between nutrients and carbon during remineralization. In the second concept, according to the results from analyses of ocean tracer data on isopycnal [*Takahashi et al.*, 1985] and neutral surfaces [*Anderson and Sarmineto*, 1994, hereinafter referred to as AS94], the remineralization ratios are approximately constant throughout the ocean because no fractionation takes place.

In the Arabian Sea a diversity of biogeochemical provinces such as eutrophic, oligotrophic, upwelling, and reducing oxygen environments arises from the unique combination of climate, circulation, and geology [*Burkhill et al.*, 1993; *Mantoura et al.*, 1993; *Swallow*, 1984]. The ventilation of the Arabian Sea intermediate and deep water is generally from south of the equator and from marginal seas as the Red Sea and the Persian Gulf. The distributions of temperature and salinity indicate intense vertical, diapycnal mixing [*Tomczak and Godfrey*, 1994], composing the complex water mass structure of the Arabian Sea. Monsoons cause complete semiannual reversals in the surface circulation of the Arabian Sea. This results in the upwelling of nitrogen-rich water along the coast of Oman and Somali, making the basin one of the most productive areas of the world's oceans [*Qasim*, 1977, 1982].

An intense oxygen minimum zone (OMZ), containing <5 μmol kg^{-1} O$_2$ is established at intermediate depth ($\sim$150-1200 m) northward 12°N and eastward 56°E [e.g., *Mantoura et al.*, 1993; *Naqvi*, 1987], which is maintained by moderate consumption in waters of initially low O$_2$ content [*Olson et al.*, 1993]. The OMZ is one of the largest denitrification sites in the global ocean and remineralization of organic matter by heterotrophic bacteria utilizing nitrate as an oxidizing agent has a major influence on the distribution of biogeochemical tracers in the Arabian Sea [e.g., *Howell et al.*, 1997; *Naqvi*, 1987; *Naqvi et al.*, 1992]. The largest nitrate deficits are certainly found in the OMZ, but advection and diffusion are responsible for the propagation of these deficits far outside the OMZ [*Gruber and Sarmiento*, 1997].

In the assessment of the remineralization ratios from oceanic chemical data, two difficulties are encountered, which have to be considered. First, the DIC concentrations in the upper and intermediate waters are contaminated with anthropogenic CO$_2$. This amount has to be eliminated from the observed DIC data if one is interested in changes of the inorganic carbon pool due to biological processes. Investigations of *Sabine et al.* [1999] and *Goyet et al.* [1999] have shown that surface waters in the Arabian Sea contain $\sim$40 μmol kg^{-1} anthropogenic CO$_2$ with a penetration depth down to $\sim$1500 m. A second task is to account for the nitrate deficits in the active denitrification sites as well as outside the OMZ owing to the advection of denitrified waters [*Gruber and Sarmiento*, 1997].

Considering both, the denitrification and the anthropogenic CO$_2$, the observed concentrations of nutrients, DIC, and oxygen should be affected by water mass mixing and remineralization processes. In this study we obtain the mixing fraction and the biogeochemical change by applying a linear inverse mixing model, the extended optimum multiparameter (OMP) analysis [*Karstensen*, 1999; *Karstensen and Tomczak*, 1998], to the observational data. Addressing the importance of diapycnal fluxes, this analysis is not restricted to certain spreading surfaces. We extend the "classical" Redfield ratios by including silicon in our results because in some regions, silicate seems to play an important role in the drawdown of atmospheric CO$_2$ via the biological pump [*Dugdale and Wilkerson*, 1998].

2. Data

Two data sets were analyzed (Figure 1), from the German R/V *Meteor* World Ocean Circulation Experiment (WOCE) expedition M32/4 (June 8 to July 10, 1995) covering the western Arabian Sea and from the U.S. R/V *Thomas G. Thompson* Joint Global Ocean Flux Study (JGOFS) expedition TTN/049 (July 18 to August 13, 1995) in the northeastern Arabian Sea, respectively. Both data sets contain potential temperature (θ), salinity (S), oxygen (O$_2$), phosphate (PO$_4^{3-}$), nitrate (NO$_3^-$), nitrite (NO$_2^-$), silicate (Si(OH)$_4$), dissolved inorganic carbon (DIC), and total alkalinity (TALK). The methods employed for the measurements and the accuracy of the analysis are according to the international WOCE and JGOFS standards [*Knap et al.*, 1996; *World Ocean Circulation Ex. (WOCE)*, 1994]. The methods of DIC and TALK analysis are explicit described by *Department of Energy (DOE)* [1994].

The bottle θ-S data (Figure 2) show the distinct influence of high-salinity water originating from the Persian Gulf (TTN/049 data; diamonds) along isopycnal 26.8 kg m^{-3}, and the Red Sea (M32/4 data; grey circles) along isopycnal 27.2 kg m^{-3}. The influence of
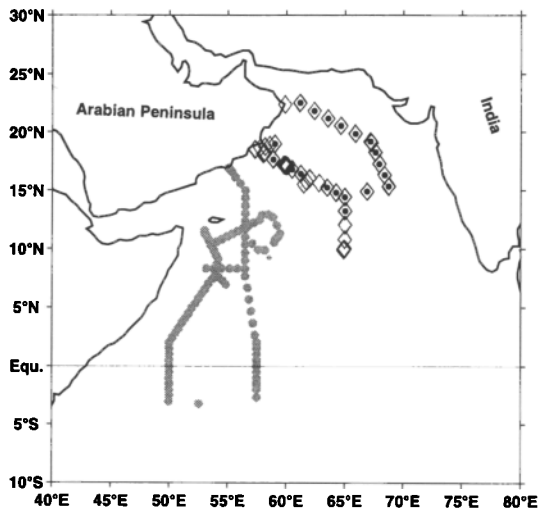
Figure 1. Position of the M32/4 (grey circles) and the TTN/049 (diamonds) cruise in the Arabian Sea. Solid dots indicate in situ denitrification at depth >500 m (oxygen is <5 μmol kg^{-1}).

the high-salinity waters down to the Indian Deep Water is evident. For comparison the θ-S values of the five source water types are represented as open squares.

The distribution of oxygen, DIC, and nutrients (PO_4^{3-}, NO_3^-, $Si(OH)_4$, NO_2^-) versus depth is shown in Figure 3 for each station in the southwestern Arabian Sea (M32/4, 4°N, 51°E) and in the central basin (TTN/049, 14.45°N, 65°E). In the central Arabian Sea the oxygen concentration rapidly decreases from approximately saturation at the surface to near zero values at the top of the OMZ ($\sim$150 m) and remains on this low level within the OMZ, while DIC and primary nutrients (PO_4^{3-}, NO_3^-) continuously increase due to the decomposition of organic matter. The low productive oligotrophic southwestern Arabian Sea is much better oxygenated at intermediate depth and an OMZ with near zero concentrations is not developed. Owing to less enrichment of remineralization products at intermediate layers DIC and nutrient concentrations are lower compared to the northern area.

As a consequence of the ventilation from the south of the Indian Ocean, the oxygen content in the deep waters increases, while nutrient concentrations slightly decrease. Despite this refreshment and the declined activity of organic matter remineralization in the deep sea, the DIC content remains approximately constant because the dissolution of calcium carbonate contributes to the DIC as well as to the TALK concentrations [*Millero et al.*, 1998]. Again, the oxygen concentrations are lower in the central basin associated with higher DIC and nutrient concentrations. The lower oxygen content and the higher amount of DIC and nutrients in the whole water column from the southwest-

ern to the northeastern Arabian Sea are attributed to the enhanced primary productivity and to the longer spreading path of the water masses. Silicate concentrations also increase with depth accompanied by higher amounts at the northernmost station. In contrast to the distribution of nitrate and phosphate the silicate maximum is found at greater depth because of the slow release during the chemical dissolution of siliceous skeletons. The suboxic conditions within the OMZ lead to a loss of nitrate by denitrification indicated by the secondary nitrite maximum ($\sim$200 m) at the central station.

The relationships between the Redfield quantities DIC, phosphate, nitrate, and AOU are depicted in Figure 4. We rather use AOU than oxygen to avoid effects of air-sea gas exchange at the sea surface. The higher the AOU, the greater the amount of O_2 removed since the water mass was last in contact with the atmosphere. Negative AOU values indicate oversaturation of the water in respect of oxygen. A bifurcation of the AOU distribution separates the upper and the lower water column regimes, with the OMZ ($\sim$150-1200 m) in between. We included "iso-Redfieldians" in the figure for the classical Redfield ratio (dashed line) and for the results of the latest comprehensive study of AS94 (solid line). These lines merely denote the remineralization slopes of both estimates to give a first impression of general trends. The AOU/PO_4^{3-} and the AOU/NO_3^- relationship reflect more the classical Redfield slope in the upper regime and the AS94 slope in the lower regime, possibly implying a change in the remineralization ratios with depth. Nitrate loss due to denitri-
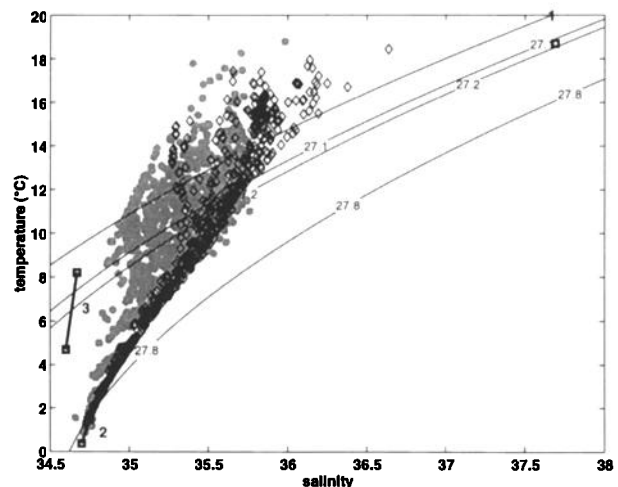

Figure 2. Potential temperature versus salinity distribution of cruises M32/4 (grey circles) and TTN/049 (diamonds) for depths >200 m. The source water types are indicated as open squares: 1, Red Sea/Persian Gulf Water (RSW/PGW); 2, upper and lower Indian Deep Water (IDW); 3, upper and lower modified Antarctic Intermediate Water (mAAIW).
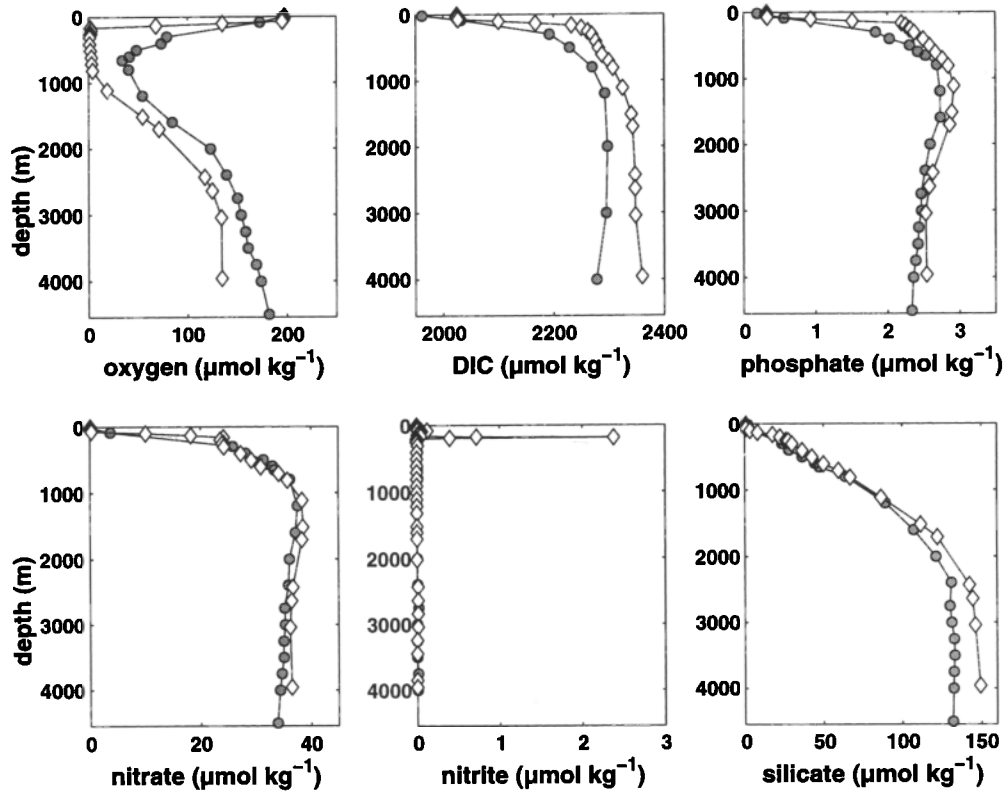
Figure 3. Typical vertical profiles of oxygen, DIC and primary nutrients in the southwestern Arabian Sea (M32/4, circles) at 4°N, 51°E and the central Arabian basin (TTN/049, diamonds) at 14.45°N, 65°E.
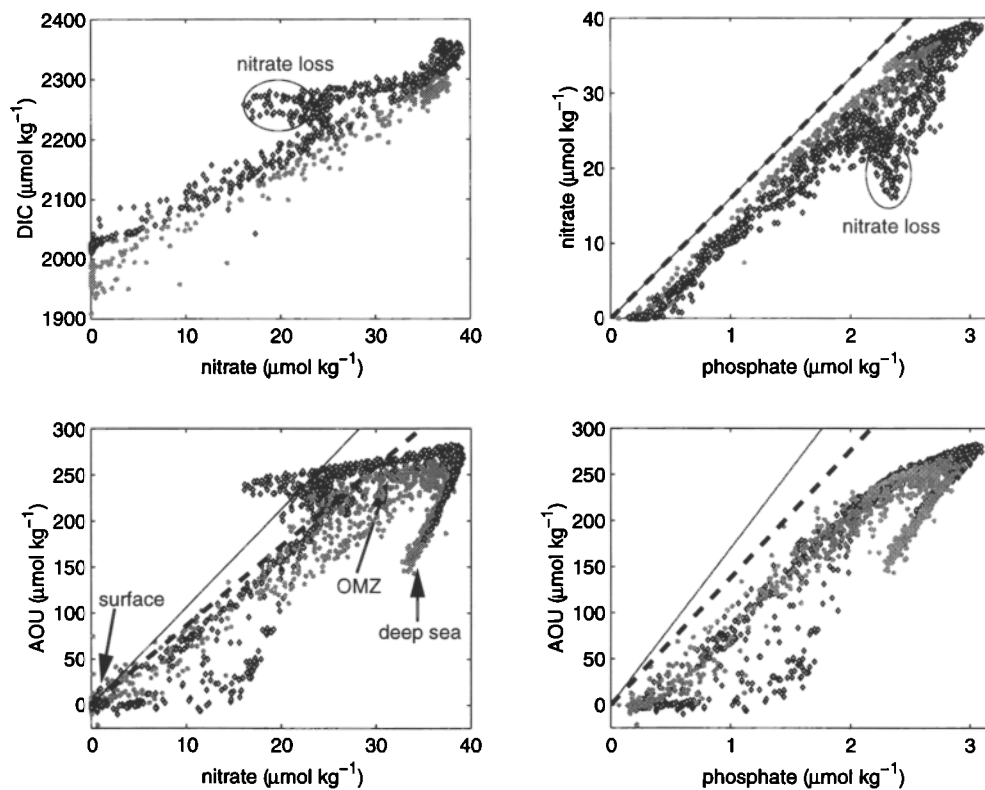

Figure 4. Property/property plots of cruises M32/4 (grey circles) and TTN/049 (diamonds). Dashed line represents the "classical" Redfield slope; solid line indicates the AS94 slope.

fication within the OMZ can be found primarily for the TTN/049 data, while an advection of denitrified water southward during the southwest monsoon season may occur, influencing also the property distribution farther south [*Gruber and Sarmiento*, 1997; *Naqvi*, 1987]. The occurrence of denitrification is best demonstrated by looking at the nitrate property plots. The DIC concentrations are affected by air-sea gas exchange at the surface, by the contamination with anthropogenic CO_2 in upper and intermediate waters and by the formation/dissolution of calcium carbonate, which decouple this tracer from nutrient concentrations. Therefore no iso-Redfieldians are included in the DIC plot.

3. Method

In this study we used a further development of a linear inverse mixing model, the extended optimum multiparameter (OMP) analysis [*Karstensen*, 1999; *Karstensen and Tomczak*, 1998] including all general mechanisms composing an observed tracer field: mixing, remineralization, denitrification, and carbon cycling. A set of tracers, temperature, salinity, oxygen, nutrients, and carbon species (DIC, TALK), is fitted to the model. The model predicts the mixing fractions of the predefined source water types, the time-integrated amount of biogeochemical changes in oxygen, the nutrients and inorganic carbon through remineralization, and the nitrate deficit due to denitrification. Our effort was to obtain reliable results for physical components (mixing fractions) as well as for biogeochemical cycling components. The basic assumption for the model is linear mixing with identical mixing coefficients, implying generally turbulent mixing.

3.1. Model Equations

We used a set of equations of the following form which is similar to the one used by AS94:

by POM degradation. The amount of nitrate removed by denitrification is included as ΔN^{deni}. Here r_D is the ratio of phosphorus remineralized for a given loss of nitrate assumed to be 0.01 obtained by coupling the reaction equation of denitrification with the remineralization of POM as composed in equation (1) [*Gruber and Sarmiento*, 1997]:.

$$C_{106}H_{175}O_{42}N_{16}P + 104\ NO_3^- \rightarrow 4\ CO_2$$
$$+102\ HCO_3^- + 60\ N_2 + 36\ H_2O + HPO_4^{2-}$$
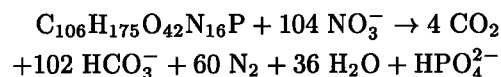
Finally, the amount of carbon added by the dissolution of calcareous material is ΔC_{inorg}. The right-hand side of the equations is given by the observational data T_{obs}, S_{obs}, $O_{2,obs}$, ... and the residuals (R_{tracer}) occurring from the solution procedure. The last row is an expression of the mass conservation of the mixing components ($\sum x_i = 1$). The main difference between our investigation and the one from AS94 is the predefinition of the source water types (T_i, S_i, $O_{2,i}$, ...). Through this, the system of equations is overdetermined, allowing a nonnegative least squares (NNLS) technique [*Lawson and Hanson*, 1974] to find the solution of the unknowns (x_i, ΔP, ΔN^{deni}, and ΔC_{inorg}). There is no restriction for certain spreading surfaces of water masses, allowing diapycnal mixing effects to compose the observational data, playing a vital role in the northern Indian Ocean [AS94; *Tomczak and Godfrey*, 1994]. A first calculation is done with a set of first guess Redfield ratios. For the ratio $r_{Si/P}$, involved in the dissolution of opaline silica, an averaged value of 40/1 is used [*Broecker and Peng*, 1982; *Takeda*, 1998; *Watson and Whitfield*, 1985].

To obtain the remineralization ratios, the analyzed mixing fraction as well as the effects of denitrification and dissolution of calcium carbonate on the thus af-

x_1T_1	$+\cdots+$	x_5T_5	$+$	0	$+$	0	$+$	0	$= T_{obs} + R_T$
x_1S_1	$+\cdots+$	x_5S_5	$+$	0	$+$	0	$+$	0	$= S_{obs} + R_S$
$x_1O_{2,1}$	$+\cdots+$	$x_5O_{2,5}$	$-$	$r_{O/P}\Delta P$	$+$	0	$+$	0	$= O_{2,obs} + R_{O_2}$
$x_1PO_{4,1}$	$+\cdots+$	$x_5PO_{4,5}$	$+$	$r_{P/P}\Delta P$	$+$	$r_D\Delta N^{deni}$	$+$	0	$= PO_{4,obs} + R_{PO_4}$
$x_1NO_{3,1}$	$+\cdots+$	$x_5NO_{3,5}$	$+$	$r_{N/P}\Delta P$	$-$	ΔN^{deni}	$+$	0	$= NO_{3,obs} + R_{NO_3}$
x_1Si_1	$+\cdots+$	x_5Si_5	$+$	$r_{Si/P}\Delta P$	$+$	0	$+$	0	$= Si_{obs} + R_{Si}$
x_1DIC_1	$+\cdots+$	x_5DIC_5	$+$	$r_{C_{org}/P}\Delta P$	$+$	$r_D r_{C_{org}/P}\Delta N^{deni}$	$+$	ΔC_{inorg}	$= DIC_{obs} + R_{DIC}$
x_1TALK_1	$+\cdots+$	x_5TALK_5	$-$	$r_{N/P}\Delta P$	$+$	ΔN^{deni}	$+$	$2\Delta C_{inorg}$	$= TALK_{obs} + R_{TALK}$
x_1	$+\cdots+$	x_5	$+$	0	$+$	0	$+$	0	$= 1 + R_\Sigma$

On the left-hand side, x_i are the five source water type fractions to compose each observational data through mixing of the predefined source water types (SWT) T_i, S_i, $O_{2,i}$, ... In the biogeochemical part of the model, the amount of phosphate added from remineralization of organic matter (ΔP) is linked via a set of first guess Redfield ratios $r_{tracer/P}$ to access the changes in the remaining biogeochemical tracers caused

fected tracer are subtracted from the observational data [*Karstensen*, 1999]. Thus the amount of biogeochemical changes for each component (-ΔO_2, ΔC_{org}, ΔN, ΔP, and ΔSi) are revealed. Relating -$\Delta O_2/\Delta P$, $\Delta C_{org}/\Delta P$, $\Delta N/\Delta P$, and $\Delta Si/\Delta P$ gives the set of ratios which was only valid if the residuals of the tracers were found to

be small (~0). Because a NNLS technique is used and several sources of errors exist (e.g., measurement errors, source water type definition errors) the residuals will never be identical to zero. On the other hand, the residuals providing a way to assess the quality of the NNLS fit [e.g., *Karstensen*, 1999; *Karstensen and Tomczak*, 1998; *You and Tomczak*, 1993].

Having a set of equations of properties with different ranges and units, a normalization has to be done before a solution of the system can be found. Because some properties are absolute values (SWT) and other are relative values (r), the normalization is split in two stages [*Karstensen*, 1999]: At first, a normalization of the subsystem composed by the absolute values, we call it G, was done. In a few words (details are given by *Tomczak and Large* [1989]), from each tracer j, say, salinity, the mean of all salinity SWT values is subtracted and afterward divided by the standard deviation of all salinity SWT values. Doing this for all tracers results in a normalized SWT matrix we want to call G'. In a second stage all relative values (r) are normalized for each tracer j in respect of G versus G' using

$$r' = \frac{(G_j)_{max} - (G_j)_{min}}{(G'_j)_{max} - (G'_j)_{min}} r$$

Finally, combining G' and r' gives the normalized matrix for which the solution vector can be found.

The uncertainties in each tracer is related to the resolvability of the tracer field in terms of tracer variability in the source water matrix (for details, see *Mackas et al.* [1987] and *Tomczak and Large* [1989]). By reason of a limited availability of data in the "source" region of our water masses, we choose a mean of the weights from earlier OMP analysis [*You*, 1998; *You and Tomczak*, 1993] using historical Indian Ocean data (Table 1, weights column). Owing to the high quality of the WOCE and JGOFS data, the chosen weights have to be seen as a lower limit. Because silicate is not directly

linked to the remineralization of POM, we decided to weight this tracer by a factor of ~10 lower than the other.

To set up the system, the source water types of the water masses in the Arabian Sea have to be defined. In general, four sources of ventilating an oceanic region are possible [*Tomczak*, 1999]: convection, subduction, internal mixing, and import of water from other regions of the world ocean. Only two of them add new tracer characteristics through air-sea interaction: convection and subduction. In general, the ventilation of the intermediate and deep layers occurs only at certain locations [*Tomczak and Godfrey*, 1994]. Thus the observed tracer concentration outside of these formation areas is a product of mixing of waters originating from these particular locations and biogeochemical cycling.

For the intermediate and deep layers of the Arabian Sea we defined three source water masses, represented by five SWT (Table 1 and Figure 2; open squares) from Geochemical Ocean Sections Study (GEOSECS) Indian Ocean data [*Weiss et al.*, 1983]: Red Sea/Persian Gulf Water (RSW/PGW), Indian Deep Water (IDW), and modified Antarctic Intermediate Water (mAAIW). All of these water masses are mixtures of other water masses. The IDW is a mixture of the convective formed sources of North Atlantic Deep Water, Weddell Sea Water, and Pacific and Indian Intermediate Water [*Emery and Meincke*, 1986]. The RSW/PGW source characteristic is formed by mixing of Red Sea Water and Persian Gulf Water with ambient water in the Gulf of Aden and the Gulf of Oman, respectively [*Banse*, 1997; *Siedler*, 1968]. The mAAIW originates from convective formed Antarctic Intermediate Water [*England et al.*, 1993], mixed with the deep Indonesian Throughflow Water [*You*, 1998]. Consequently, the SWT definition values (Table 1) are not "preformed" values in oxygen, carbon properties, and nutrients in a biogeochemical sense. Anyway, defining the sources

Table 1. Source Water Types for OMP Analysis as Defined With GEOSECS Indian Ocean Data

	IDW		RSW/PGW	mAAIW		Weights
	Upper	Lower		Upper	Lower	
Temperature °C	1.47	0.38	18.70	8.20	4.70	24
Salinity	34.75	34.70	37.69	34.67	34.60	24
O_2, $\mu mol\,kg^{-1}$	202	216	50	144	97	5
PO_4^{3-}, $\mu mol\,kg^{-1}$	2.07	2.20	1.56	1.87	2.48	5
NO_3^-, $\mu mol\,kg^{-1}$	30.4	32.1	19.7	26.5	37.6	5
$Si(OH)_4$, $\mu mol\,kg^{-1}$	110.0	125.3	19.2	31.5	99.0	0.5
DIC, $\mu mol\,kg^{-1}$	2240	2256	2172	2170	2281	5
TALK, $\mu mol\,kg^{-1}$	2356	2358	2364	2294	2356	5

IDW, Indian Deep Water; RSW, Red Sea Water; PGW, Persian Gulf Water; mAAIW, modified Antarctic Intermediate Water.
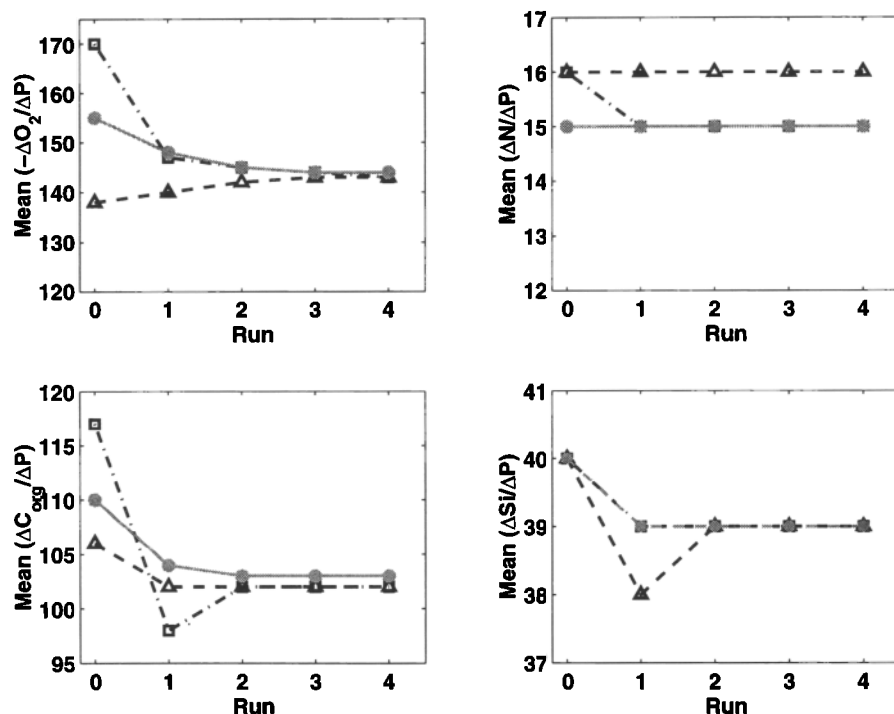
Figure 5. Influence of first guess ratios on the mean values of analyzed remineralization ratios. *Redfield et al.* [1963] (triangles), AS94 (squares), and mean values (grey circles).

"upstream" relative to the investigated region allows the assumption that the whole tracer field "downstream" is composed by them. On the other hand, the "nonpreformed" definition restricts our results to be relative values referred to the SWT only. To ensure that the changes in the biogeochemical tracers are significantly higher than the measurement errors, all source water types are defined far outside the Arabian Sea. Additionally, the investigated depth range (550-4500 m) is assumed to be unaffected by surface processes as upwelling or mixing with upwelled water.

3.2. Evaluation of Error Sources

The influence of three potential sources of errors on the estimated remineralization ratios are examined: the first guess ratio ($r_{O/P}$, $r_{Si/P}$, $r_{N/P}$, $r_{C_{org}/P}$, $r_{P/P}$), the variabilities through shortcomings in the source water types definitions (G_j) and the data (measurement errors), and the effect of anthropogenic carbon.

The impact of the first guess remineralization ratios was proven iteratively. Starting with an initial guess ratio (run zero) gave a set of new ratios, which are used as input for the next run and so on (Figure 5). Three sets of first guess ratios were used: the classical ratios (triangles [*Redfield et al.*, 1963]), the AS94 ratios (squares), and something in between (grey circles), while value of 40 for $r_{Si/P}$ has been retained unchanged. It was found that at least after the second run, the following mean ra-

tios differed only slightly from the former. Ultimately, all choices of initial remineralization ratios converged to the same result. This shows that the OMP analysis is quite insensitive to the first guess of ratios. The results presented later are the ratios derived from the second run using the ratios $r_{C_{org}/P}/r_{N/P}/r_{P/P}/-r_{O/P}$ as 110/15/1/155.

The stability of the results with regard to the variability of the source water masses and the measurement accuracy of the tracers is examined by adding 100 times random noise on both simultaneously. For the SWT we choose an error of ±10% on the anomaly relative to the Indian Deep Water (Figure 6). This was done assuming that the IDW has a very low variability. The measurement noise was of the order of the standard deviation for the appropriate observational tracer. The impact of the noise on the results is indicted as a standard deviation on our results (see section 4). Systematic deviations in the residuals from a zero mean value are corrected through slight changes in the source water-type definition values.

Because our model does not include the effect of anthropogenic CO_2 on the DIC observations, we corrected the data before analyzing it. Defining an exponential function adapted for the results of a recent study in the Arabian Sea by *Sabine et al.* [1999] provides anthropogenic CO_2 concentrations of about 21, 8, 3, and 1 μmol kg^{-1} in depths of 500, 750, 1000, and 1500 m,
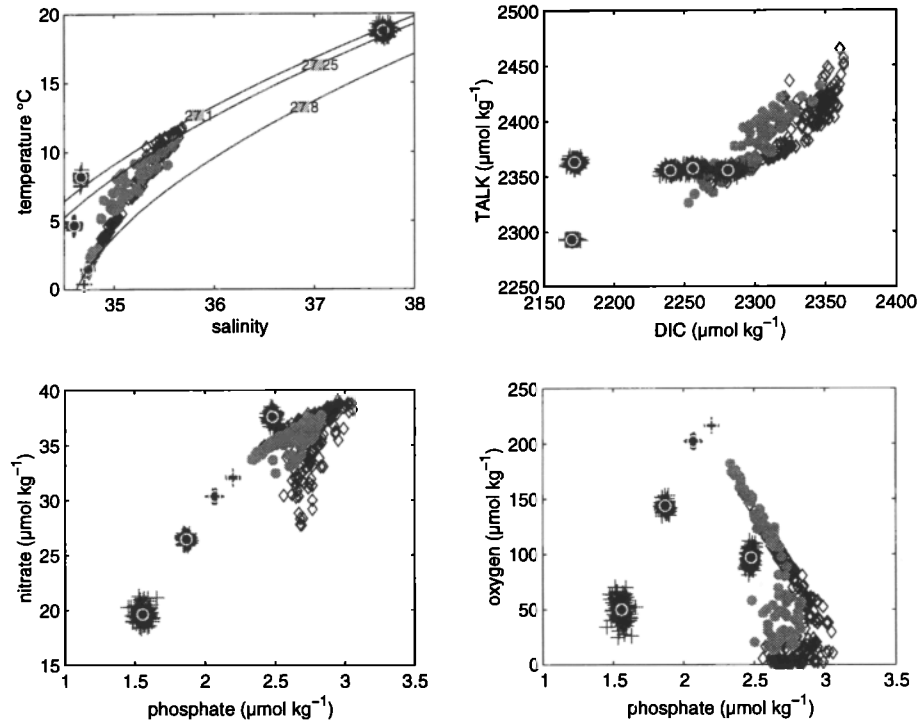
Figure 6. Variability of source water types by adding 100 times random noise (pluses) in position to observational data (M32/4, grey circles; TTN/049, diamonds).

respectively. Additionally, we used values lowered by a factor of 2 as an approach to the findings from *Goyet et al.* [1999]. They used a multiparameter method to determine water mass fractions combined with a parameterized remineralization term to quantify the amount of anthropogenic CO_2. Applying both corrections to our data improved our results in terms of lower residuals (Figure 7). Anyway, the changes in the stoichiometric ratios through the correction is within the error margins.

It is worth noting here that the extended OMP analysis can be used to calculate the anthropogenic CO_2 by iteratively finding the best correction on the DIC values in respect to R_{DIC}, but this is beyond the scope of the present study. Moreover, the low-quality DIC data of the GEOSECS program are not sufficient to determine the small amounts of anthropogenic CO_2 below 500 m with adequate accuracy.

4. Results and Discussion

In Figures 8-16 the standard deviation on all results presented in this section is obtained by adding 100 times random noise on source water types and observational data simultaneously.

4.1. Water Mass Fractions

The depth dependency of the water mass fractions from both cruises is shown in Figure 8. As already sug-

gested from looking at the θ/S data, the influence of RSW/PGW is quite deep, down to 2000 m. Starting as a single point in the tracer space (Table 1), this indicates enhanced vertical, diapycnal mixing. Highest fractions can be found at 550 m depth in the northern TTN/049 data related to the proximity of the Persian Gulf outflow into the Arabian Sea. The signal gets more diluted with the mAAIW as one goes farther to the south (M32/4 data). A second peak at ~1000 m depth in the M32/4 data indicates the influence of Red Sea Water. Modified Antarctic Interme-
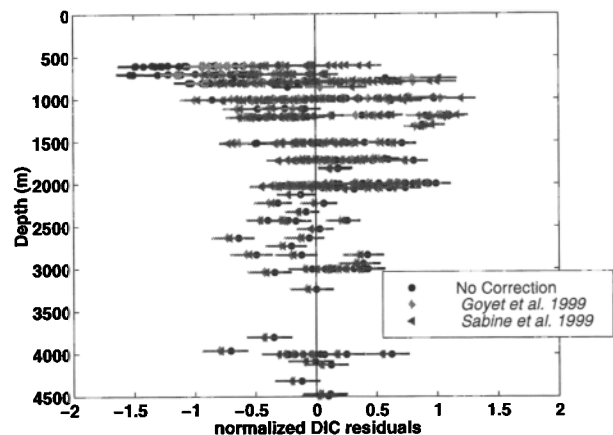

Figure 7. The influence of anthropogenic CO_2 corrections on the residuals of DIC (R_{DIC}).
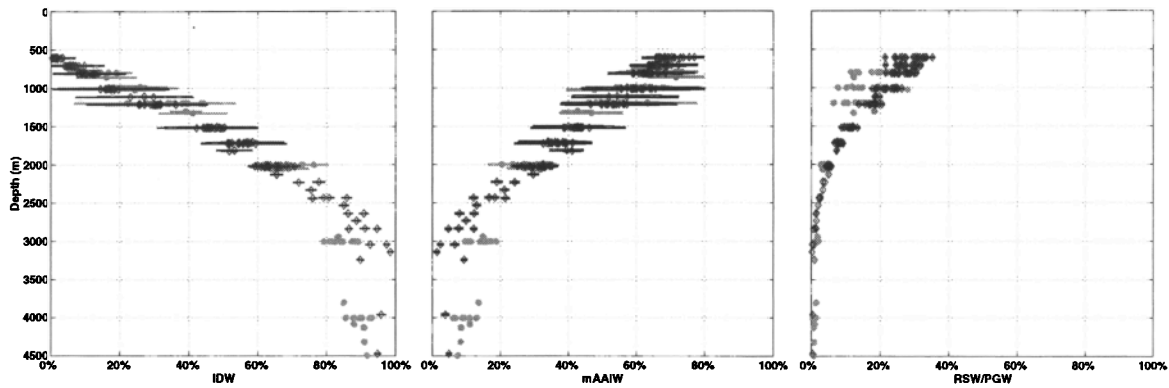
Figure 8. Water mass fractions of predefined source water masses. Indian Deep Water (IDW), modified Antarctic Intermediate Water (mAAIW), and Red Sea/Persian Gulf Water (RSW/PGW).

diate Water (mAAIW) enters the Arabian Sea from the south, as can be seen in slightly higher concentrations in the M32/4 data (grey circles). It gets diluted with RSW/PGW while travelling northward. The influence of the Indian Deep Water (IDW) increases nearly linear to 100% at ~3000 m depth in both data sets.

4.2. Denitrification

The variable ΔN^{deni} in the model represents the amount of nitrate removed by denitrification. The values are composed by in situ denitrification within the OMZ as well as by advection of denitrified waters to outside the minimum layer. As can be seen in Figure 9a, ΔN is highest in the active denitrification sites of the OMZ in the northeastern Arabian Sea (solid dots in Figure 1) and decreases with depth and toward the southwest because these sites are effected by advection of nitrate deficits rather than by in situ denitrification. The peak values of ΔN^{deni} (~8 μmol kg^{-1}) at 550 m are in good agreement with the results of *Mantoura et al.*

[1993] calculating the nitrate deficits in the northern Arabian Sea along 67°E. Basically, ΔN^{deni} is the deviation from the linear $\Delta N/\Delta P$ ratio; therefore it is comparable to N* from *Gruber and Sarmiento* [1997, p.241] (Figure 9b) within the error margins (solid lines) calculated from their equation (17).

4.3. Remineralization Ratios

Figures 10 to 16 show the means of the remineralization ratios for M32/4 (grey circles) and TTN/049 (diamonds) versus depth, as well as the standard deviation (error bars). The ratios of AS94 in the Indian Ocean (solid stars) and the "classical" Redfield ratios (dashed line) are included for comparison.

The mean -$\Delta O_2/\Delta P$ ratios (Figure 10) of both cruises are approximately Redfieldian (139 ± 7) within the OMZ (550-1200 m). The values increase to 152 ± 5 below the OMZ until 2000 m depth. In the deep sea (depth >2000 m) we find constant -$\Delta O_2/\Delta P$ ratios of about 160. Some values above 160 are reached in the
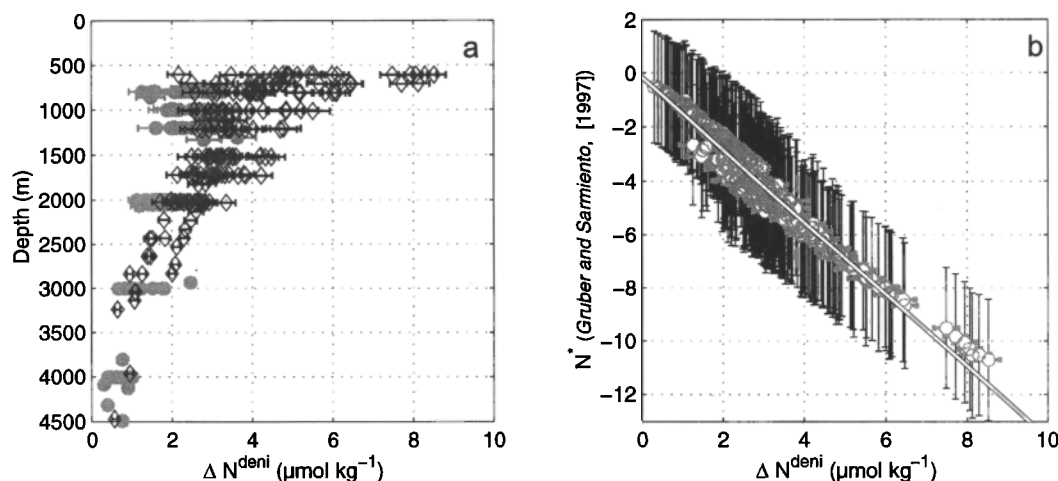

Figure 9. (a) Depth dependency of ΔN^{deni} caused by in situ denitrification and advection of denitrified waters. (b) ΔN^{deni} versus N* with best linear fit and appropriate error bars.
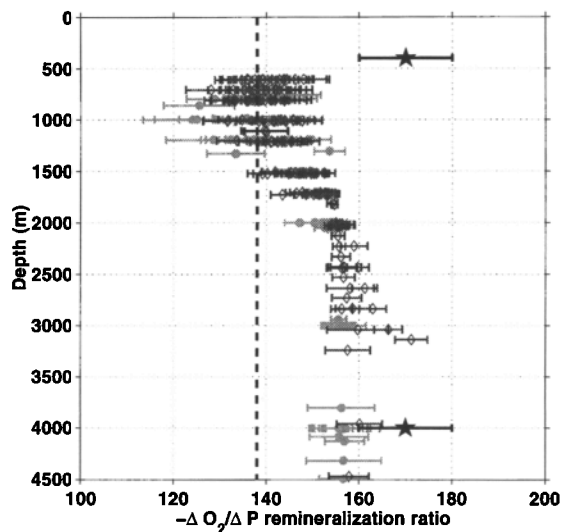
Figure 10. The $-\Delta O_2/\Delta P$ remineralization ratios versus depth of M32/4 (grey circles) and TTN/049 (diamonds). For comparison, the ratio of AS94 in the Indian Ocean (solid stars) as well as the classical Redfield ratio (dashed line) are included.

deep northeastern Arabian Sea (TTN/049). The oxygen utilization of $-\Delta O_2$ in this study is equivalent to the AOU in the biogeochemical sense, but the calculation is different. Hence the problems of supersaturated surface waters and the nonlinearity in the solubility of oxygen associated to the reliable estimation of the AOU [e.g., *Broecker and Peng*, 1982] do not occur in determining the $-\Delta O_2$ values. In general, our results do not reflect the assumption of constant remineralization ratios with depth. We obtained $-\Delta O_2/\Delta P$ ratios, which are generally coinciding with the classical Redfield ratio of 138 in intermediate waters and nearly correspond to the constant values of 170 determined by AS94 in deep waters. The anomaly of 200 at 1000 m found by AS94 for the Indian Ocean could not be validated by our results. As AS94 used a two end-member model in the Indian Ocean between 400 and 2000 m (a southern component mixing with Arabian Sea Water), they attributed this anomaly rather to the mixing of a third end-member from the Indonesian Archipelago than to biogeochemical processes, as confirmed by our results.

The $\Delta C_{org}/\Delta P$ estimates reveal a strong depth dependency (Figure 11). Essentially, low ratios of 90 ± 9 are reached within the OMZ, while the values increase to 107 ± 8 down to 2000 m. Toward the deep sea, the ratios further increase, attaining within the error bars a constant mean value of 127 ± 12 below 2000 m. The continuous rise from low estimates within the OMZ to high values in deep waters suggests that organic phosphorus is more reactive than organic carbon and is thus remineralized more rapidly. This is consistent with

lower $-\Delta O_2/\Delta P$ values in the OMZ and higher ratios in the deep sea, since most oxygen is consumed during organic carbon respiration. The ratios for the deep sea are, however, in excellent agreement with the recent estimates of *Millero et al.* [1998] in the upper waters of the Arabian Sea ($\Delta C_{org}/\Delta P = 125$). The low values in the depth range 550-1200 m are similar to the $\Delta C_{org}/\Delta P$ ratios of 81 (100 m) and 99 (1000 m) found by *Shaffer* [1996] for the global ocean. Furthermore, they are in reasonable agreement with the $\Delta C_{org}/\Delta P$ estimates of ~ 100 in 750 m reported by *Shaffer et al* [1999] for the low- and midlatitude Pacific, Indian, and South Atlantic Oceans. As mentioned in section 3.2, the observed DIC concentrations are corrected due to the effect of anthropogenic CO_2 before analysis. Therefore the thermocline ratios should be not biased by this perturbation.

A closer consideration of the Indian Ocean $\Delta C_{org}/\Delta P$ estimates of AS94 reveals a quite good conformity to our distribution pattern in the deep sea but to a lesser extent at intermediate layers. However, because of the large error bars on their calculations, owing to inaccurate DIC measurements in the Indian Ocean, they derived a $\Delta C_{org}/\Delta P$ ratio of 117 ± 14 throughout the water column using their constant $-\Delta O_2/\Delta P$ result of 170 ± 10 combined with an assumed $-\Delta O_2/\Delta C_{org}$ ratio of 1.45 ± 0.15. The latter is the mean value of the photosynthetic quotient of 1.4 ± 0.1 [*Laws*, 1991] and an $-\Delta O_2/\Delta C_{org}$ ratio of 1.6 for organic detritus [*Martin et al.*, 1987]. The application of values between 1.3 and 1.6 produces $\Delta C_{org}/\Delta P$ remineralization ratios somewhere between 103 and 131. Accordingly, small deviations from this assumed mean $-\Delta O_2/\Delta C_{org}$ ratio lead
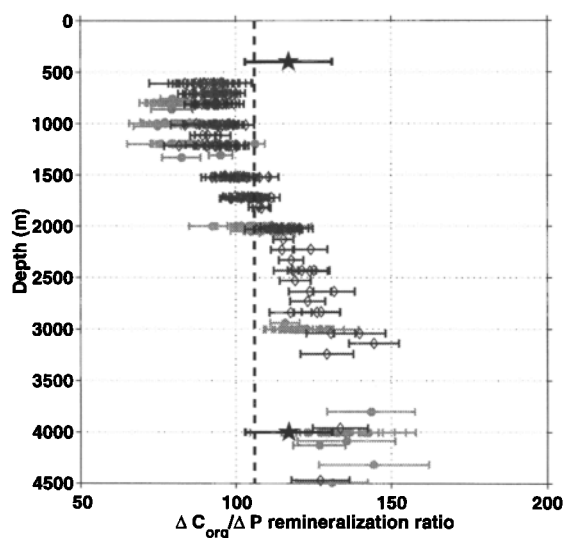

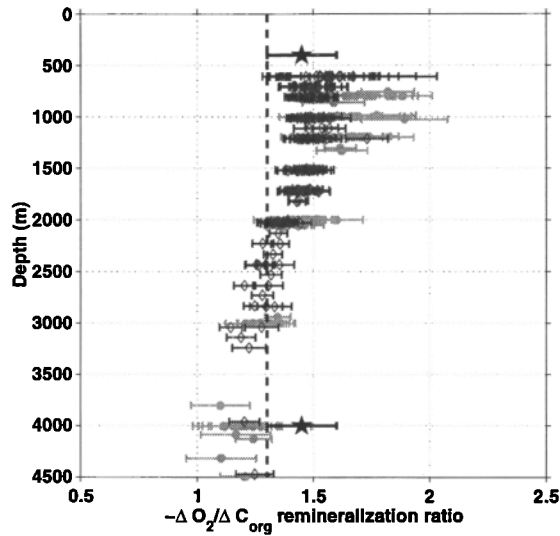**Figure 11.** The $\Delta C_{org}/\Delta P$ remineralization ratios versus depth of both cruises. Symbols and lines are explained in Figure 10.

Figure 12. The $-\Delta O_2/\Delta C_{org}$ remineralization ratios versus depth of both cruises. Symbols and lines are explained in Figure 10.

to significant changes in the $\Delta C_{org}/\Delta P$ estimates. The $-\Delta O_2/\Delta C_{org}$ ratio of 1.6 is probably the upper limit, because *Martin et al.* [1987] neglect the oxygen content of organic matter (AS94), but values below 1.3 are absolutely accessible in the Arabian Sea (*Millero et al.* [1998], compare Figure 12).

The $-\Delta O_2/\Delta C_{org}$ ratios (Figure 12) decrease from an average of 1.56 ± 0.15 in the OMZ to 1.43 ± 0.08 down to 2000 m. In the deep sea (depth >2000 m) the decline of the estimates is continued to 1.25 ± 0.11. The steady decrease of the $-\Delta O_2/\Delta C_{org}$ ratios with depth indicates that lipids or proteins are preferentially remineralized at

intermediate depth, while the degradation of higher oxidized compounds like carbohydrates is taking place in the deeper Arabian Sea. Whether the differences in the thermocline ratios ($\Delta C_{org}/\Delta P$, $-\Delta O_2/\Delta C_{org}$) between both cruises reflect regional aspects or not is ambiguous yet.

The $\Delta N/\Delta P$ ratios (Figure 13) vary between 14.4 ± 0.2 in intermediate waters (550-1200 m) to 15.3 ± 0.2 in the deep sea (depth >2000 m). Overall, the variation in the $\Delta N/\Delta P$ remineralization ratios with depth is not strongly developed, and we think neither phosphate nor nitrate is remineralized preferentially. It is worth mentioning that our calculated $\Delta N/\Delta P$ ratios are lower than the classical value of 16 throughout the water column, which is supported by investigations of *Morrison et al.* [1998]. Therefore it would appear that the effect of denitrification is exceeding the effect of nitrogen fixation, even though the Indian Ocean is known as a site of enhanced N_2 fixation [e.g., *Carpenter*, 1983]. Considering the findings of *Morrison et al.* [1998] and *Mantoura et al.* [1993], our $\Delta N/\Delta P$ ratios < 16 suggest that primary production in the Arabian Sea is limited by nitrate rather than by phosphate availability.

Our value of 14.4 ± 0.2 in the OMZ is in reasonable agreement with the overall ratio of 13.53 from *Millero et al.* [1998]. The middepth minimum ($\Delta N/\Delta P = 12$) observed by AS94 in the Indian Ocean is not confirmed by our results ($\Delta N/\Delta P \sim 15$ at 1000-3000 m). In an earlier version of the model we performed a correction on nitrate and phosphate data for in situ denitrification coupled with the oxygen content. In so doing, we also found such low ratio values between 10 and 12 at middepth because this correction failed to account for
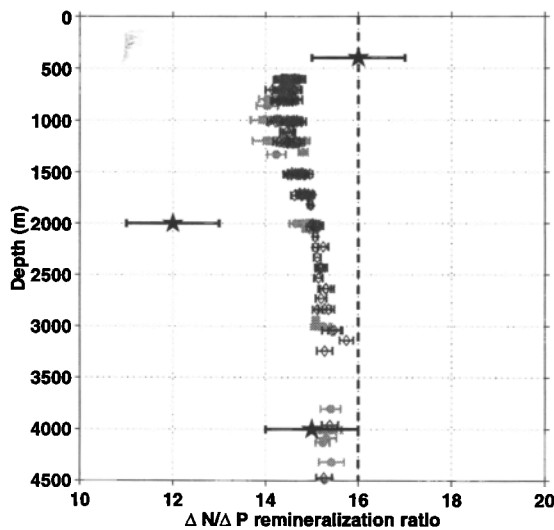

Figure 13. The $\Delta N/\Delta P$ remineralization ratios versus depth of both cruises. Symbols and lines are explained in Figure 10.

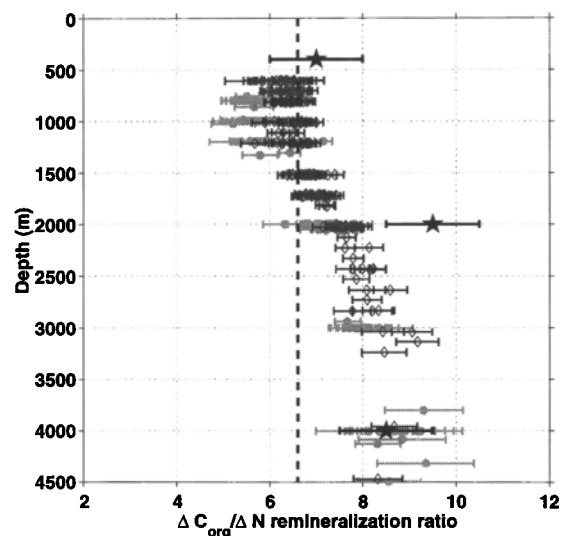**Figure 14.** The $\Delta C_{org}/\Delta N$ remineralization ratios versus depth for both cruises. Symbols and lines are explained in Figure 10.

the advection of water masses with a nitrogen deficit produced upstream [e.g., *Gruber and Sarmiento*, 1997]. Owing to the integration of the denitrification term in the model equations, the analysis is considered for the in situ denitrification in the OMZ as well as for advection and mixing with denitrified waters. *Naqvi* [1987] pointed out that horizontal advection and diffusion are responsible for the export of >85% of the nitrate deficits mainly through the southern boundary. In the deep sea our results correspond to the $\Delta N/\Delta P$ ratios of AS94.

The CO_2 uptake by the photosynthetic organisms is assessed by converting the biological changes of NO_3^- into the biological changes of DIC with reference to the $\Delta C_{org}/\Delta N$ remineralization ratio (Figure 14). The $\Delta C_{org}/\Delta N$ results are somewhat lower in the OMZ (6.2 ± 0.5) than the classical Redfield ratio of 6.6. Furthermore, the ratios increase up to a mean value of 7.2 ± 0.5 below the OMZ until 2000 m. In the deep Arabian Sea down to 4500 m the estimates further increase to 8.3 ± 0.7, which is in good agreement with the findings of AS94. Assuming an export production with the typical elementary composition of surface ocean phytoplankton as determined by *Fleming* [1940], the continuously increasing $\Delta C_{org}/\Delta N$ ratios with depth suggest that nitrate like phosphate is regenerated more rapidly and therefore more shallowly from the sinking POM than DIC. However, the sinking fluxes of particulate organic carbon are inadequate for meeting the carbon demand within the intermediate waters because the zone of intense subsurface denitrification is characterized by low primary production in the overlying surface waters [*Ducklow*, 1993; *Naqvi and Shailaja*, 1993; *Naqvi et al.*, 1992]. *Naqvi et al.* [1993] have proposed that the advective and diffusive transports of dissolved organic carbon from the surface layer could plausibly form an important source of carbon for microbial metabolism within the denitrifying layer.

In addition to the carbon added from the oxidation of organic matter (C_{org}), DIC contains an amount added from the dissolution of calcium carbonate (C_{inorg}). This fraction is calculated by implementing the total alkalinity corrected for the release of nitrate in the model equations. The $\Delta C_{org}/\Delta C_{inorg}$ ratio gives information about the regenerated carbon stemming from organic/inorganic sources and, moreover, allows a conclusion about the composition of the sinking material.

The $\Delta C_{org}/\Delta C_{inorg}$ ratios (Figure 15) rapidly decrease from ~4 ± 1 at 550 m to 2 ± 0.2 at 2000 m, reaching 1.2 ± 0.3 at 4000 m depth. The distribution of the $\Delta C_{org}/\Delta C_{inorg}$ ratios with depth points out that remineralization of organic residues occurs, on the average, at shallower depth than the dissolution of calcium carbonate. The estimates further suggest that at least below 550 m the dissolution of $CaCO_3$ is significant. The Arabian Sea is thought to be supersaturated with re-
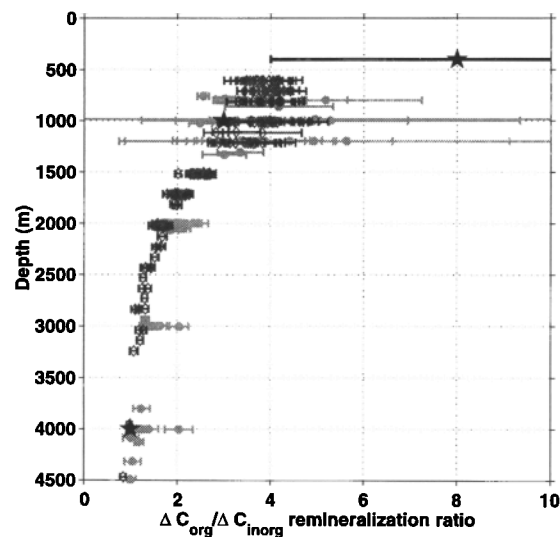

Figure 15. The $\Delta C_{org}/\Delta C_{inorg}$ remineralization ratios versus depth of both cruises. Symbols and lines are explained in Figure 10.

spect to aragonite and calcite above 600 m and 3400 m, respectively [e.g., *Anderson and Dyrssen*, 1994; *Millero et al.*, 1998]. The values of nearly 4 in the upper section of the OMZ in the Arabian Sea are conspicuously lower than the estimates of roughly 12 in the South Atlantic at 400 m [*Takahashi et al.*, 1985]. This higher degree of $CaCO_3$ dissolution in the northwestern Indian Ocean is favored by high values of CO_2 partial pressure (pCO_2) in the OMZ exceeding 1000 μatm [*George et al.*, 1994; *Millero et al.*, 1998]. The pronounced maximum in pCO_2 is attributed to autochthonous organic matter decomposition in the OMZ as well as to the advection of waters carrying enhanced pCO_2 values owing to remineralization activities since leaving the source regions. Furthermore, the $\Delta C_{org}/\Delta C_{inorg}$ ratios suggest that already 20% of the carbon regenerated within the OMZ and even 45% of the carbon released at 4000 m is from skeletal $CaCO_3$ dissolution. The results also reveal regional aspects, especially in the deeper layers, with generally higher values in the western Arabian Sea (M32/4) and lower regeneration ratios in the northern Arabian Sea (TTN/049). Presumably, the deep northern Arabian Sea is the most corrosive to calcium carbonate.

$CaCO_3$ is the major constituent of downward particle flux in the Arabian Sea contributing 35-70% to bulk fluxes [*Haake et al.*, 1993; *Nair et al.*, 1989]. The only reason that significant amounts of calcium carbonate are dissolved above the calcite lysocline is that this $CaCO_3$ is in form of aragonite. Pteropods, aragonite-shelled organisms, accumulate in shallow sediment traps at 1000 m depth, whereas only small numbers are counted in deep traps at 3000 m (V. Ittekkot, personal
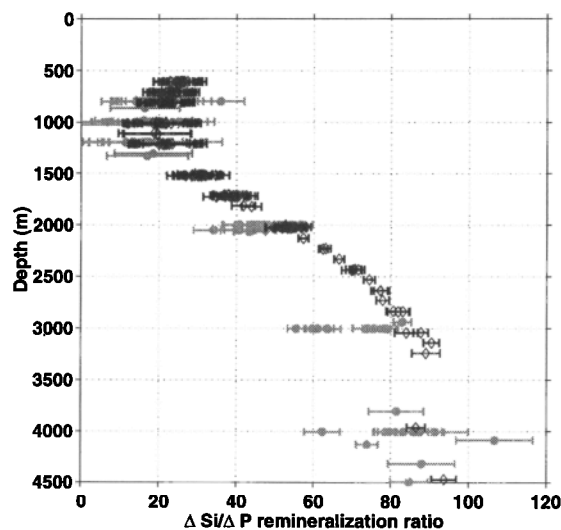
Figure 16. The $\Delta Si/\Delta P$ remineralization ratios versus depth of both cruises. Symbols and lines are explained in Figure 10.

communication, 1999). The signal of $CaCO_3$ corrosion in the Arabian Sea at intermediate depth seems to be primarily due to the dissolution of aragonite, as suggested by recent investigations of *Millero et al.* [1998].

The $\Delta Si/\Delta P$ ratios (Figure 16) generally increase with depth. Between 550 and 1200 m the ratios are approximately constant at a value of 21 ± 9, but they increase up to $\sim 72 \pm 10$ at 3000 m. The $\Delta Si/\Delta P$ ratios are highest below 4000 m (84 ± 11). Silicon is, in contrast to nitrogen and phosphorus, not part of the organic soft tissue, but silicate is, in addition to nitrate and phosphate, an essential nutrient for silica-shelled phytoplankton such as diatoms. The opal fluxes in the western Arabian Sea, mostly in form of diatoms, account for up to 22% of the total annual flux of POM [*Nair et al.*, 1989]. In contrast to $CaCO_3$, the entire water column is undersaturated with respect to opaline silica. However, as the chemical dissolution of biogenic silica shells is rather slow in comparison with the microbial degradation of organic matter, silicate is regenerated at greater depth than nitrate or phosphate. The poorer recycling efficiency causes a greater degree of horizontal and vertical segregation of silicate. The strong increase of the $\Delta Si/\Delta P$ remineralization ratios with depth is mainly attributed to the slower dissolution of opaline silica, which is dependent on the thermodynamic driving force compared to the remineralization of organic phosphorus. In addition, the silicate concentration is more affected by other sources as advection of silicate derived from dissolution of surface sediments from the shelf region [*Rixen et al.*, 1999] or river input (e g., Indus). This may account for conspicuously lower ratios below 2000 m depth in M32/4 data compared to

TTN/049. The calculated remineralization ratios are summarized in Table 2.

4.4. Depth Dependency of the POM Remineralization in the Water Column

In general, 40-60% of the carbon in marine phytoplankton is in the form of proteins. Carbohydrates and lipids compose 20-40% and 5-20% of the cellular carbon, respectively [*Libes*, 1992]. It is obvious from generally low $\Delta C_{org}/\Delta P$ and $-\Delta O_2/\Delta P$ ratios within the OMZ that organic phosphorus compounds are preferentially remineralized in the upper water column. On the other hand, the higher $-\Delta O_2/\Delta C_{org}$ ratios found in the OMZ likewise hint at the degradation of higher hydrogenated carbon compounds such as proteins or especially lipids, which requires more oxygen to oxidize both carbon and hydrogen [e.g., *Anderson*, 1995; *Takahashi et al.*, 1985]

$$CH_2 + 1.5\,O_2 \rightleftharpoons CO_2 + H_2O$$
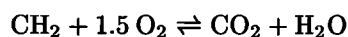
than it would require to oxidize carbohydrates with higher oxygen contents [*Redfield et al.*, 1963]:

$$CH_2O + O_2 \rightleftharpoons CO_2 + H_2O.$$
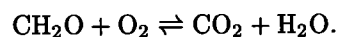
One possible explanation is the remineralization of phospholipids, a major component of planktonic cell walls. The lower $\Delta C_{org}/\Delta P$ ratios within the OMZ suppose the preferential decomposition of nucleic acids like energy-carrying molecules such as ATP and NADP or RNA and DNA, which store and transmit genetic information within cells. Nucleic acids contribute to the cell nitrogen content as well.

Considering the N-related remineralization ratios, one can suppose that the high $-\Delta O_2/\Delta C_{org}$ ratios in the OMZ are additionally maintained by the degradation of proteins. The lower $\Delta C_{org}/\Delta N$ ratios in the OMZ in comparison to the deep waters may indicate the release of both carbon and nitrogen due to the degradation of proteins and nucleic acids . In summary, we suggest that in the upper 1500 m phosphorus and nitrogen-rich compounds such as phospholipids and nucleic acids as well as proteins are remineralized preferentially.

In the deeper Arabian Sea between 2000 and 4500 m more carbon and less phosphorus are remineralized, as indicated by high $\Delta C_{org}/\Delta P$ and $-\Delta O_2/\Delta P$ ratios, compared to in the thermocline. Obviously, the composition of organic carbon decomposed in the deeper waters have changed, supported by low averaged $-\Delta O_2/\Delta C_{org}$ values of 1.25. We therefore presume the remineralization of organic carbon predominantly in the form of more oxidized carbohydrates and a reduction in protein decomposition indicated by high $\Delta C_{org}/\Delta N$ ratios in the deep sea. Altogether we assume that the organic matter remineralized in the deep Arabian Sea has high $\Delta C_{org}/\Delta N$ and $\Delta C_{org}/\Delta P$ ratios. Our results

Table 2.   Averaged Remineralization Ratios for Both Cruises Determined With the OMP Analysis in the Arabian Sea.

Ratio	Depth Range		
	550-1200 m (OMZ)	1200-2000 m	2000-4500 m
$-\Delta O_2/\Delta P$	139 ± 7	152 ± 5	158 ± 5
$\Delta N/\Delta P$	14.4 ± 0.2	14.9 ± 0.2	15.3 ± 0.2
$\Delta C_{org}/\Delta P$	90 ± 9	107 ± 8	127 ± 12
$\Delta C_{org}/\Delta N$	6.2 ± 0.5	7.2 ± 0.5	8.3 ± 0.7
$-\Delta O_2/\Delta C_{org}$	1.56 ± 0.15	1.43 ± 0.08	1.25 ± 0.11
$\Delta C_{org}/\Delta C_{inorg}$	4 ± 1.2	2 ± 0.4	1.3 ± 0.3
$\Delta Si/\Delta P$	21 ± 9	43 ± 10	78 ± 11

are consistent to the $\Delta C_{org}/\Delta N$ and $\Delta C_{org}/\Delta P$ ratios found in POM caught in sediment traps of the Pacific and Atlantic Oceans, which tend to increase with depth [e.g., *Honjo and Manganini*, 1993; *Honjo et al.*, 1982; *Martin et al.*, 1987].

5. Summary and Conclusions

The remineralization ratios of Arabian Sea subsurface waters between 550 and 4500 m are determined using a linear inverse mixing model, the extended optimum multiparameter analysis. We applied this method to hydrographic, nutrient, and carbon data of two cruises sampled in the Arabian Sea in 1995 to separate the mixing fractions of predefined source water types from the amount of biogeochemical changes at a given bottle data point integrated over the spreading path. The method accounts for the effects of denitrification, and the contaminated DIC concentrations are corrected for the amount of anthropogenic CO_2 before analysis.

The resulting mean $\Delta C_{org}/\Delta N/\Delta P/-\Delta O_2$ remineralization ratios are not constant throughout the water column but rather reveal a dependency on depth. In the OMZ (550-1200 m) we found estimates of $90\pm9/14.4\pm0.2/1/139\pm7$, which increase to values of $107\pm8/14.9\pm0.2/1/152\pm5$ down to 2000 m. In the deep sea (depth >2000 m) the ratios are approximately constant at $127\pm12/15.3\pm0.2/1/158\pm5$. The $\Delta N/\Delta P$ estimates in the whole water column of the Arabian Sea are slightly lower than the Redfield ratio of 16. This suggests that the effects of denitrification are dominating the effects of N_2 fixation, making this region of the ocean a potential sink for fixed nitrogen.

The vertical fractionation during remineralization found above 2000 m is in agreement with the findings of *Shaffer* [1996] and *Shaffer et al.* [1999], even though both studies are based on different views of biogeochemical cycling in the ocean. *Shaffer* [1996] concludes that the vertical uniformity of ocean rem-

ineralization ratios, as reported by AS94 or *Takahashi et al.* [1985], is the consequence of neglecting diapycnal mixing in the intermediate layers of the ocean, an effect that is considered in the OMP analysis. Furthermore, the $\Delta C_{org}/\Delta N/\Delta P/-\Delta O_2$ remineralization ratios of this study are generally lower than those estimated by AS94 in the upper 2000 m, while they are in reasonable agreement with the constant values of AS94 in the deep sea below 2000 m. We suppose that phosphate and nitrate are released in the mean faster than carbon dioxide during remineralization indicated by noticeable higher $\Delta C_{org}/\Delta P$ and $\Delta C_{org}/\Delta N$ ratios in the deeper Arabian Sea.

The $\Delta C_{org}/\Delta C_{inorg}$ estimates suggest the dissolution of calcium carbonate at depth conspicuously above the calcite lysocline. This feature is apparently attributed to the corrosion of aragonite-shelled pteropods. The skeletal $CaCO_3$ dissolution accounts for 20 and 45% of the carbon regenerated in the OMZ (550-1200 m) and at 4000 m, respectively. The $\Delta Si/\Delta P$ ratio is approximately constant in the OMZ (21 ± 9) and rapidly increases with depth to 72 ± 10 at 3000 m. In the Arabian Sea the $\Delta Si/\Delta P$ ratio seems to be convenient to upgrade the Redfield stoichiometry.

We hope this work encourages the use of multitracer analysis in biogeochemistry. It offers a way to take into account transport and biogeochemical cycling as composing mechanisms for the observed tracer field.

References

Anderson, L., and D. Dyrssen, Alkalinity and total carbonate in the Arabian Sea: Carbonate depletion in the Red Sea and Persian Gulf, *Mar. Chem.*, *47*, 195–202, 1994.

Anderson, L. A., On the hydrogen and oxygen content of marine phytoplankton, *Deep Sea Res.*, *42*, 1675–1680, 1995.

Anderson, L. A., and J. L. Sarmiento, Redfield ratios of remineralization determined by nutrient data analysis, *Global Biogeochem. Cycles*, *8*, 65–80, 1994.

Banse, K., Irregular flow of Persian (Arabian) Gulf water to the Arabian Sea, *J. Mar. Res.*, *55*, 1049–1067, 1997.

Brewer, P. G., Direct observation of the oceanic CO₂ increase, *Geophys. Res. Lett.*, *5*, 997–1000, 1978.

Broecker, W. S., 'NO', a conservative water-mass tracer, *Earth Planet. Sci. Lett.*, *23*, 100–107, 1974.

Broecker, W. S., and T.-H. Peng, *Tracers in the Sea*, Lamont-Doherty Geol. Obs., Palisades, N.Y., 1982.

Burkhill, P. H., R. F. C. Mantoura, and N. J. P. Owens, Biogeochemical cycling in the northwestern Indian Ocean: A brief overview, *Deep Sea Res.*, *40*, 643–649, 1993.

Carpenter, E. J., Nitrogen fixation by marine *oscillatoria* (Trichodesmium) in the world's oceans, in *Nitrogen in the Marine Environment*, edited by E. J. Carpenter and D. Capone, pp. 65–103, Academic, San Diego, Calif., 1983.

Copin-Monteguet, C., and G. Copin-Monteguet, Stoichiometry of carbon, nitrogen and phosphorus in marine particulate matter, *Deep Sea Res.*, *30*, 31–46, 1983.

Department of Energy (DOE), *Handbook of Methods for the Analysis of the Various Parameters of the Carbon Dioxide System in Sea Water*, edited by A. G. Dickson and C. Goyet, version 2, *Rep. ORNL/CDIAC-74*, 1994.

Ducklow, H. W., Bacterioplankton distributions and production in the northwestern Indian Ocean and Gulf of Oman, September 1986, *Deep Sea Res.*, *40*, 753–771, 1993.

Dugdale, R. C., and F. P. Wilkerson, Silicate regulation of new production in the equatorial Pacific upwelling, *Nature*, *391*, 270–273, 1998.

Emery, W. J., and J. Meincke, Global water masses: summary and review, *Océanol. Acta*, *9*, 383–391, 1986.

England, M. H., J. S. Godfrey, A. C. Hirst, and M. Tomczak, The mechanism for Antarctic Intermediate Water renewal in a world ocean model, *J. Phys. Oceanogr.*, *23*, 1553–1560, 1993.

Fleming, R. H., The composition of plankton and units for reporting population and production, *Proceedings of the 6th Pacific Science Congress, Calif., 1939*, vol. 3, pp. 535–540, 1940.

George, M. D., M. D. Kumar, S. W. A. Naqvi, S. Banerjee, P. V. Narvekar, S. N. de Sousa, and D. A. Jayakumar, A study of the carbon dioxide system in the northern Indian Ocean during premosoon, *Mar. Chem.*, *47*, 243–254, 1994.

Goyet, C., C. Coatanoan, G. Eischeid, T. Amaoka, K. Okuda, R. Healy, and S. Tsunogai, Spatial variations of total CO₂ and total alkalinity in the northern Indian Ocean: A novel approach for the quantification of anthropogenic CO₂ in seawater, *J. Mar. Res.*, *57*, 135–163, 1999.

Gruber, N., and J. L. Sarmiento, Global patterns of marine nitrogen fixation and denitrification, *Global Biogeochem. Cycles*, *11*, 235–266, 1997.

Gruber, N., J. L. Sarmiento, and T. F. Stocker, An improved method for detecting anthropogenic CO₂ in the oceans, *Global Biogeochem. Cycles*, *10*, 809–837, 1996.

Haake, B., V. Ittekkot, T. Rixen, V. Ramswamy, R. R. Nair, and W. B. Curry, Seasonality and interannual variability of particle fluxes to the deep Arabian Sea, *Deep Sea Res.*, *40*, 1323–1344, 1993.

Honjo, S., and S. J. Manganini, Annual biogenic particle fluxes to the interior of the North Atlantic Ocean: Studied at 34°N 21°W and 48°N 21°W, *Deep Sea Res.*, *40*, 587–607, 1993.

Honjo, S., S. J. Manganini, and J. J. Cole, Sedimentation of biogenic matter in the deep ocean, *Deep Sea Res.*, *29*, 609–625, 1982.

Howell, E. A., S. C. Doney, R. A. Fine, and D. B. Olson, Geochemical estimates of denitrification in the Arabian Sea and the Bay of Bengal during WOCE, *Geophys. Res. Lett.*, *24*, 2549–2552, 1997.

Karstensen, J., The extended OMP analysis, *Tech. Rep. 1-99*, Inst. für Meereskunde, Univ. of Hamburg, Hamburg, Germany, 1999.

Karstensen, J., and M. Tomczak, Age determination of mixed water masses using CFC and oxygen data, *J. Geophys. Res.*, *103*, 18,599–18,610, 1998.

Knap, A., A. Michaels, A. Close, H. Ducklow, and A. Dickson (Eds.), *Protocols for the Joint Global Ocean Flux Study (JGOFS) Core Measurements*, Reprint of the IOC Manuals and Guides 29, UNESCO, 1994, *JGOFS Rep. 19*, vi+170 pp, 1996.

Knauer, G. A., J. H. Martin, and K. W. Bruland, Fluxes of particulate carbon, nitrogen and phosphorus in the upper water column of the northeast Pacific, *Deep Sea Res.*, *26*, 445–462, 1979.

Laws, E. A., Photosynthetic quotients, new production and net community production in the open ocean, *Deep Sea Res.*, *38*, 143–167, 1991.

Lawson, C. L., and R. J. Hanson, *Solving Least Square Problems*, Prentice-Hall, Englewood Cliffs, N.J., 1974.

Libes, S. M., *An Introduction to Marine Biogeochemistry*, 734 pp., John Wiley, New York, 1992.

Mackas, D. L., K. L. Denman, and A. F. Bennett, Least squares multiple tracer analysis of water mass composition, *J. Geophys. Res.*, *92*, 2907–2918, 1987.

Maier-Reimer, E., Geochemical cycles in an ocean general circulation model: Preindustrial tracer distributions, *Global Biogeochem. Cycles*, *7*, 645–677, 1993.

Mantoura, R. F. C., C. S. Law, N. J. P. Owens, P. H. Burkhill, E. M. S. Woodward, R. J. M. Howland, and C. A. Lewellyn, Nitrogen biogeochemical cycling in the northwestern Indian Ocean, *Deep Sea Res.*, *40*, 651–671, 1993.

Martin, J. H., G. A. Knauer, D. M. Karl, and W. W. Broenkow, VERTEX: Carbon cycling in the northeast Pacific, *Deep Sea Res.*, *34*, 267–285, 1987.

Millero, F. J., E. A. Degler, D. W. O'Sullivan, C. Goyet, and G. Eischeid, The Carbon Dioxide System in the Arabian Sea, *Deep Sea Res.*, *45*, 2225–2252, 1998.

Minster, J.-F., and M. Boulahdid, Redfield ratios along isopycnal surfaces - a complementary study, *Deep Sea Res.*, *34*, 1981–2003, 1987.

Morrison, J. M., L. A. Codispoti, S. Gaurin, B. Jones, V. Manghnani, and Z. Zheng, Seasonal variation of hydrographic and nutrient fields during the US JGOFS Arabian Sea Process Study, *Deep Sea Res.*, *45*, 2053–2101, 1998.

Nair, R. R., V. Ittekkot, S. J. Manganni, V. Ramaswamy, B. Haake, E. T. Degens, B. N. Desai, and S. Honjo, In-

creased particle flux to the deep ocean related to monsoons, Nature, 338, 749–751, 1989.

Naqvi, S. W. A., Some aspects of the oxygen-deficient conditions and denitrification in the Arabian Sea, J. Mar. Res., 45, 1049–1072, 1987.

Naqvi, S. W. A., and M. S. Shailaja, Activity of the respiratory electron transport system and respiration rates within the oxygen minimum layer of the Arabian Sea, Deep Sea Res., 35, 687–695, 1993.

Naqvi, S. W. A., R. J. Noronha, M. S. Shailaja, K. Somasundar, and R. Sen Gupta, Some aspects of the nitrogen cycling in the Arabian Sea, in Oceanography of the Indian Ocean, edited by B. N. Desai, pp. 285–311, Oxford & IBH Publishing, New Delhi, 1992.

Naqvi, S. W. A., M. D. Kumar, P. V. Narvekar, S. N. de Sousa, M. D. George, and C. D'Silva, An intermediate nepheloid layer associated with high microbial metabolic rates and denitrification in the Northwest Indian Ocean, J. Geophys. Res., 98, 16,469–16,479, 1993.

Olson, D. B., G. L. Hitchcock, R. A. Fine, and B. A. Warren, Maintenance of the low-oxygen layer in the central Arabian Sea, Deep Sea Res., 40, 673–685, 1993.

Parsons, T. R., M. Takahashi, and B. Hargrave, Biological Oceanographic Processes, Pergamon, Tarrytown, N.Y., 1984.

Qasim, S. Z., Biological productivity of the Indian Ocean, Indian J. Mar. Sci., 6, 122–137, 1977.

Qasim, S. Z., Oceanography of the northern Arabian Sea, Deep Sea Res., 29, 1041–1068, 1982.

Redfield, A. C., B. H. Ketchum, and F. A. Richards, The Influence of Organism on the Composition of Sea Water, in The Sea, vol. 2, edited by M. N. Hill, pp. 26–77, Wiley-Interscience, New York, 1963.

Rixen, T., B. Haake, and V. Ittekkot, Sedimentation in the western Arabian Sea: The role of coastal and open-ocean upwelling, Deep Sea Res., in press, 1999.

Sabine, C. L., R. M. Key, K. M. Johnson, F. J. Millero, A. Poisson, J. L. Sarmiento, D. W. R. Wallace, and C. D. Winn, Anthropogenic CO_2 inventory of the Indian Ocean, Global Biogeochem. Cycles, 13, 179–198, 1999.

Sambrotto, R. N., et al., Elevated consumption of carbon relative to nitrogen in the surface ocean, Nature, 363, 248–250, 1993.

Shaffer, G., Biogeochemical cycling in the global ocean, 2, New production, Redfield ratios, and remineralization in the organic pump, J. Geophys. Res., 101, 3723–3745, 1996.

Shaffer, G., J. Bendtsen, and O. Ulloa, Fractionation during remineralization of organic matter in the ocean, Deep Sea Res., 46, 185–204, 1999.

Siedler, G., Schichtungs- und Bewegungsverhältnisse am Südausgang des Roten Meeres, "Meteor" Forschungsergeb., Reihe A 4, 1–76, 1968.

Swallow, J. C., Some aspects of the physical oceanography of the Indian Ocean, Deep Sea Res., 31, 639–650, 1984.

Takahashi, T., W. S. Broecker, and S. Langer, Redfield ratio based on chemical data from isopycnal surfaces, J. Geophys. Res., 90, 6907–6924, 1985.

Takeda, S., Influence of iron availability on nutrient consumption ratio of diatoms in oceanic waters, Nature, 393, 774–777, 1998.

Toggweiler, J. R., Carbon overconsumption, Nature, 363, 210–211, 1993.

Tomczak, M., Some historical, theoretical and applied aspects of quantitative water mass analysis, J. Mar. Res., 57, 275–303, 1999.

Tomczak, M., and S. Godfrey, Regional Oceanography: An Introduction, 422 p., Pergamon, Tarrytown, N.Y., 1994.

Tomczak, M., and D. G. B. Large, Optimum multiparameter analysis of mixing in the thermocline of the eastern Indian Ocean, J. Geophys. Res., 94, 16,141–16,149, 1989.

Watson, A. J., and M. Whitfield, Composition of particles in the global ocean, Deep Sea Res., 32, 1023–1039, 1985.

Weiss, R. F., W. S. Broecker, H. Craig, and D. Spencer, Hydrographic Data 1977-1978, GEOSECS Indian Ocean Expedition, vol. 5, U.S. Govt. Print. Off., Washington, D.C., 1983.

World Ocean Circulation Ex. (WOCE), Operation manual, WHP operations and methods, part 3.1.3, WHP Off. Rep. WHPO91-1, WOCE Rep. 68/69, rev. 1, Woods Hole Oceanographic Institution, Woods Hole, Mass., 1994.

You, Y., Intermediate water circulation and ventilation of the Indian Ocean derived from water-mass contributions, J. Mar. Res., 65, 1029–1067, 1998.

You, Y., and M. Tomczak, Thermocline circulation and ventilation in the Indian Ocean derived from water mass analysis, Deep Sea Res., 40, 13–56, 1993.

A. Hupe, Institut für Biogeochemie und Meereschemie der Universität Hamburg, Bundesstr. 55, 20146 Hamburg, Germany. (hupe@geowiss.uni-hamburg.de)

J. Karstensen, Institut für Meereskunde der Universität Hamburg, Troplowitzstr. 7, 22529 Hamburg, Germany. (karstens@ifm.uni-hamburg.de)